Biochimica et Biophysica Acta 1822 (2012) 1238–1246

Contents lists available at SciVerse ScienceDirect

Biochimica et Biophysica Acta

journal homepage: www.elsevier.com/locate/bbadis

Familial hemiplegic migraine type 1 mutations W1684R and V1696I alter G protein-mediated regulation of $Ca_V2.1$ voltage-gated calcium channels

Edgar Garza-López [a], Alejandro Sandoval [b], Ricardo González-Ramírez [c], María A. Gandini [a], Arn Van den Maagdenberg [d,g], Michel De Waard [e,f], Ricardo Felix [a,*]

[a] Department of Cell Biology, Center for Research and Advanced Studies of the National Polytechnic Institute (Cinvestav-IPN), Mexico City, Mexico
[b] School of Medicine FES Iztacala, National Autonomous University of Mexico (UNAM), Tlalnepantla, Mexico
[c] Department of Molecular Biology and Histocompatibility, "Dr. Manuel Gea González" General Hospital, Mexico City, Mexico
[d] Department of Human Genetics, Leiden University Medical Centre, Leiden, The Netherlands
[e] Grenoble Institute of Neuroscience, Inserm U836 Bâtiment Edmond J. Safra, Grenoble, France
[f] University Joseph Fourier, Grenoble, France
[g] Department of Neurology, Leiden University Medical Centre, Leiden, The Netherlands

ARTICLE INFO

Article history:
Received 28 February 2012
Received in revised form 10 April 2012
Accepted 12 April 2012
Available online 20 April 2012

Keywords:
Migraine
Familial hemiplegic migraine
FHM-1
Calcium channel
G-protein regulation

ABSTRACT

Familial hemiplegic migraine type 1 (FHM-1) is a monogenic form of migraine with aura that is characterized by recurrent attacks of a typical migraine headache with transient hemiparesis during the aura phase. In a subset of patients, additional symptoms such as epilepsy and cerebellar ataxia are part of the clinical phenotype. FHM-1 is caused by missense mutations in the *CACNA1A* gene that encodes the pore-forming subunit of $Ca_V2.1$ voltage-gated Ca^{2+} channels. Although the functional effects of an increasing number of FHM-1 mutations have been characterized, knowledge on the influence of most of these mutations on G protein regulation of channel function is lacking. Here, we explored the effects of G protein-dependent modulation on mutations W1684R and V1696I which cause FHM-1 with and without cerebellar ataxia, respectively. Both mutations were introduced into the human $Ca_V2.1\alpha_1$ subunit and their functional consequences investigated after heterologous expression in human embryonic kidney 293 (HEK-293) cells using patch-clamp recordings. When co-expressed along with the human μ-opioid receptor, application of the agonist [D-Ala2, N-MePhe4, Gly-ol]-enkephalin (DAMGO) inhibited currents through both wild-type (WT) and mutant $Ca_V2.1$ channels, which is consistent with the known modulation of these channels by G protein-coupled receptors. Prepulse facilitation, which is a way to characterize the relief of direct voltage-dependent G protein regulation, was reduced by both FHM-1 mutations. Moreover, the kinetic analysis of the onset and decay of facilitation showed that the W1684R and V1696I mutations affect the apparent dissociation and reassociation rates of the Gβγ dimer from the channel complex, suggesting that the G protein-Ca^{2+} channel affinity may be altered by the mutations. These biophysical studies may shed new light on the pathophysiology underlying FHM-1.

1. Introduction

Migraine is a disabling neurovascular disorder that affects ~20% of the general population [1]. The disease is characterized by recurrent attacks of severe headache and associated autonomic symptoms, such as nausea and vomiting as well as photo- and phonophobia. In about one-third of the patients, the headache is preceded by transient focal neurological symptoms (aura). Although migraine etiology and genetic influences at the population level are unknown, recent genome-wide association studies have identified the first gene variants for migraine. These findings connect a disturbed neuronal glutamate signaling with the pathophysiology of the disease [2,3].

Until now, the molecular insights on migraine pathophysiology came from studies on familial hemiplegic migraine (FHM), a monogenic subtype of migraine with aura. FHM can be considered a model for common migraine, because attacks in FHM patients are very similar to those in the common types, except for a long-lasting hemiparesis during the aura phase [4,5], and also because the FHM patients may exhibit migraine attacks with or without aura. Likewise, in FHM patients the clinical phenotype can also include epilepsy and/or cerebellar abnormalities ranging from nystagmus to progressive mild ataxia [6,7]. Three genes are known to be associated with FHM. Mutations in *CACNA1A* and *SCN1A*, encoding the ion-conducting subunits of the neuronal voltage-gated P/Q-type Ca^{2+} ($Ca_V2.1\alpha_1$) and Na^+ ($Na_V1.1$) channels, are responsible for FHM types 1 and 3

* Corresponding author at: Departamento de Biología Celular, Cinvestav-IPN, Avenida IPN #2508, Colonia Zacatenco, Mexico D.F., CP 07300, Mexico. Tel.: +52 55 57 47 39 88; fax: +52 55 57 47 33 93.
E-mail address: rfelix@cell.cinvestav.mx (R. Felix).

0925-4439/$ – see front matter © 2012 Elsevier B.V. All rights reserved.
doi:10.1016/j.bbadis.2012.04.008

(FHM-1; FHM-3), respectively, whereas mutations in ATP1A2, coding the α2 subunit of the Na^+–K^+ ATPase, are responsible for FHM-2 [5,7–10].

The functional consequences of 13 of the 21 FHM-1 mutations in the *CACNA1A* gene have been tested for their consequences on Ca^{2+} channel function using electrophysiology in heterologous expression systems [8–11]. These studies have shown that the mutations alter different properties of the human $Ca_V2.1$ channel. For instance, an enhanced channel open probability and increased single channel calcium influx associated to a shift to lower voltages of channel activation has been reported in HEK-293 cells and in $Ca_V2.1\alpha_1$ *null* neurons transfected with FHM-1 mutant $Ca_V2.1$ channels [12,13]. Likewise, a decreased density of functional channels and a consequent decreased maximal whole-cell Ca^{2+} current density has also been reported for many FHM-1 mutants [12–14]. Investigation of the functional consequences of FHM-1 gene mutations R192Q and S218L in transgenic knock-in mice [15,16], revealed increased whole cell current densities, which are in line with single channel measurements, as well as increased cortical glutamatergic neurotransmitter release [17], indicating that FHM-1 mutations more likely exert channel gain-of-function [10,11].

Much less is known, however, regarding the effects of FHM-1 mutations on the modulation of $Ca_V2.1$ channels by G proteins. Although no FHM-1 mutation has been found in the channel region involved in G-protein binding, initial studies revealed a reduction of G-protein-mediated channel inhibition by specific FHM-1 mutations [18–20], an effect that may lead to altered Ca^{2+} influx through mutant channels during neuromodulation. Here, we studied the functional consequences of two FHM-1 mutations (W1684R and V1696I) located in the fourth repeat domain of the $Ca_V2.1\alpha_1$ subunit on G-protein-mediated inhibition. Our results show that both mutants might have compromised G-protein coupling.

2. Materials and methods

2.1. Cell culture, cDNA clones and transfection

Human embryonic kidney 293 (HEK-293) cells (ATCC, Manassas, VA) were maintained in Dulbecco's modified essential medium-high glucose supplemented with 10% horse serum, 1% L-glutamine, 110 mg/L sodium pyruvate and antibiotics, at 37 °C in a 5% CO_2–95% air humidified atmosphere. Gene transfer was performed using Lipofectamine Plus reagent (Invitrogen, Carlsbad, CA) as described previously [19]. Briefly, for a 35-mm Petri dish of HEK-293 cells, 2 μg of the plasmid cDNA encoding the WT or the mutant variants of the human $Ca_V2.1$ (P/Q-type) Ca^{2+} channel pore-forming subunit splice isoform 1A-2 (GenBank accession number AF004883) [21]; in combination with 2 μg cDNA of the rat brain $Ca_V\beta_3$ (M88751) [22]; and 2 μg cDNA coding the WT rat brain $Ca_V\alpha_2\delta$-1b cDNA (M86621) [23] were premixed with 6 μL of Lipofectamine in 100 μL serum-free medium according to the manufacturer's instructions. The solution was then added to the dish and cells grown at 37 °C for 24 h, when medium was changed.

FHM-1 mutations were introduced into the human full-length cDNA encoding the $Ca_V2.1\alpha_1$ subunit of the neuronal $Ca_V2.1$ (P/Q-type) Ca^{2+} channel as previously described [24]. Mutant PCR products harboring either mutation W1684R or V1696I were subcloned into a mammalian expression vector, and sequences were verified by DNA sequencing. The cDNA coding for the human μ-opioid receptor (hMOR; AY521028) was obtained from the UMR cDNA Resource Center www.cdna.org and used as previously reported [19,25].

2.2. SDS-PAGE and Western blots

Total extracts from transfected HEK-293 cells as well as from mouse brain (used as control), were prepared as described elsewhere [26,27]. Briefly, cells were harvested, washed twice with PBS and homogenized during 20 min in cold lysis buffer (50 mM Tris–HCl pH 8.0, 150 mM NaCl, 0.5 mM PMSF, 1% of Triton X-100 and 1× complete—Roche Applied Science). Homogenized samples were clarified by a 12,000×*g* centrifugation step for 2 min. The supernatant was stored at −70 °C. Aliquots of 100 μg of protein were mixed with sample buffer (50 mM Tris–HCl, 1.7% SDS, 5% glycerol, and 0.002% bromophenol blue) and boiled for 5 min. Samples were subjected to 10% SDS-PAGE electrophoresis and proteins were transferred to a nitrocellulose membrane (Hybond-N; GE Healthcare, Buckinghamshire, UK). After blocking with non-fat milk (5%) in TBS-T (100 mM Tris–HCl, 0.15 M NaCl, 0.05% Tween 20), membranes were incubated overnight with the primary anti-hMOR antibody (Invitrogen; Cat. # 44-308G) 1:1000 in TBS-T with 5% non-fat milk, washed in TBS-T, incubated with horseradish peroxidase goat anti-rabbit secondary antibody and developed with the Immobilon Western Chemiluminescent HRP Substrate (Millipore) according to the manufacturers' instructions.

2.3. Electrophysiological recordings

Ionic currents from HEK-293 cells were recorded 48 h after transfection at room temperature (~22 °C) using the whole-cell configuration of the patch-clamp technique [28]. Ba^{2+} was used as the charge carrier. The extracellular solution contained (in mM): $BaCl_2$, 10; TEA-Cl, 125; HEPES, 10; and glucose, 10 [pH 7.3]. The intracellular solution contained (in mM): CsCl, 110; $MgCl_2$, 5; EGTA, 10; HEPES, 10; Na-ATP, 4; and GTP, 0.1 [pH 7.3]. Recordings were performed using an Axopatch 200B amplifier (Axon Instruments, Foster City, CA). Currents were digitized at a sampling rate of 5.7 kHz and filtered at 2 kHz (four-pole Bessel filter). Linear leak and parasitic capacitance components were subtracted on-line using a P/4 protocol. Membrane capacitance (C_m) was determined as previously described [29] and used to normalize currents.

2.4. Data analysis

Current–voltage (*I–V*) relationships were obtained by step depolarization between −50 mV and +70 mV in 10 mV increments, from a holding potential (V_h) of −80 mV. To assess steady-state inactivation properties, a 2-s conditioning pulse to various potentials preceded a test depolarization to +10 mV. Inactivation curves were fitted with a Boltzmann function $I_{Ba} = I_{max}/(1+\exp[(V_m - V_{1/2})/k])$, where the current amplitude (I_{Ba}) has decreased to a half-amplitude at $V_{1/2}$ with an *e*-fold change over *k* mV. Current remaining was measured from an average of 3 individual sweeps per recording using the equation: $I_{rem} = 100*(I_{end}/I_{peak})$, where I_{rem} is the current remaining at the end of a 140-ms test pulse, I_{end} is the value at the end of the test pulse, and I_{peak} is the maximum current measured during the test pulse. Time constant (τ) of inactivation was obtained from single exponential fits of I_{Ba} decaying phase using 140-ms test pulse to +10 mV.

The voltage-dependence of I_{Ba} inhibition by the G-protein Gβγ dimer was examined by applying a family of 25-ms pulses to various voltages (between −50 mV and +70 mV in 10 mV steps) 500 ms after (P1) and 5 ms before (P2) a 50-ms conditioning prepulse to +100 mV, from a V_h of −80 mV. Facilitation at different voltages was then determined as the ratio I_{Ba} (P2/P1). Facilitation decay and development (Gβγ reassociation and dissociation to the $Ca_V2.1$ channel, respectively) was studied as previously reported [18,20] applying a three-pulse voltage protocol (Fig. 3A). Facilitation decay was estimated applying two 25-ms test pulses (P1 and P2) to +10 mV separated by a conditioning prepulse to +100 mV (PP), and varying the time between PP and P2 (from 5 to 45 ms). Facilitation development was studied using a similar three-pulse voltage protocol varying the duration of the conditioning prepulse (from 2 to 15 ms).

Plots of I_{Ba} (P2/P1) as a function of time were fitted to single exponentials in order to obtain the corresponding time constants (τ).

The time constant of dissociation and re-association (τ_{off} and τ_{on}) were estimated by fitting the data to monoexponential equations of the form: $P2/P1 = 1 + I_{max}[1 - \exp(-\Delta t/\tau_{off})]$ or $P2/P1 = 1 + I_{max}[\exp(-\Delta t/\tau_{on})]$, respectively, where P1 and P2 are the maximum currents before and after the strong depolarizing prepulse, $1 + I_{max}$ is the maximum ratio of facilitation and Δt is the interpulse duration or prepulse duration, respectively.

2.5. Structural modeling of the segments S4 and S5 of domain IV in the $Ca_V2.1\alpha_1$ subunit

Homology models of transmembrane segments IVS4 and IVS5 as well as the S4–S5 linker domain (residues 1653–1710) in the $Ca_V2.1\alpha_1$ subunit were generated using the Robetta server (http://robetta.bakerlab.org). The structure of the Shaker potassium $K_V1.2$ channel model [30] was used as a template. Five models were generated and validated using the Structural Analysis and Verification Server (http://nihserver.mbi.ucla.edu/SAVES/Info.php) and the model with the best quality parameters was chosen for analysis. Computational methods for assigning partial charges and determining electrostatic potentials were applied using the Swiss-PdbViewer software (http://www.expasy.org/spdbv/). Electrostatic potentials and free energies were obtained by using a method based on the full nonlinear solution of the Poisson–Boltzmann equation [31].

3. Results

The neuronal $Ca_V2.1$ Ca^{2+} (P/Q-type) channel contains a pore-forming $Ca_V2.1\alpha_1$ (formerly α_{1A}) subunit and several regulatory subunits including $Ca_V\alpha_2\delta$ and $Ca_V\beta$. The $Ca_V2.1\alpha_1$ subunit consists of four repeated domains (I–IV) each containing six transmembrane regions (S1–S6), voltage sensors in S1–S4 and a pore loop between S5 and S6. The two FHM-1 mutations studied here (W1684R and V1696I) are located in conserved regions of the S4–S5 loop of repeated domain IV and S5 segment of domain IV, respectively (Fig. 1A). Though seminal work by Müllner and co-workers revealed that W1684R and V1696I FHM-1 mutations expressed in *Xenopus* oocytes alter $Ca_V2.1$ channel gating and these changes depended on the $Ca_V\beta$ subunit associated to the channel complex [24], the authors did not address the question of mutant-induced changes in G-protein regulation.

We first characterized the impact of W1684R and V1696I FHM-1 mutations on current density and to this end, we transiently expressed $Ca_V2.1\alpha_1$ channels in HEK-293 cells along with $Ca_V\beta_3$ and $Ca_V\alpha_2\delta$-1 auxiliary subunits, and whole-cell Ba^{2+} currents (I_{Ba}) were recorded 2 days after transfection. The presence of the mutations was verified by DNA sequencing (Suppl. Fig. 1). I_{Ba} densities resulting from expression of mutant W1684R and V1696I FHM-1 mutations were decreased in comparison with current density recorded in WT $Ca_V2.1$ channels (Fig. 1B). The potential for half-maximal activation was shifted ~5 mV to hyperpolarized potentials for the W1684R mutant channels, without changing the steepness of the I–V curve or the apparent reversal potential (Fig. 2). Likewise, the half-maximal voltage for steady-state inactivation induced by conditioning prepulses ranging −110 to +50 mV was right-shifted ~5 mV in both W1684R and V1696I channels (Fig. 1C). Such an effect was accompanied by a significant slowdown in I_{Ba} decay during a 140-ms test pulses evoked from a V_h of −80 mV to +10 mV. To quantify this effect, inactivation time constants (τ_{inact}) were obtained by fitting a single-exponential function to the decaying phases of $Ca_V2.1$ currents. W1684R and V1696I mutations increased τ_{inact} ~2-fold, and in consequence the current remaining at the end of the depolarizing pulse was also significantly increased (Fig. 1D).

Given that leftward shifts in voltage-dependence of activation and slowed inactivation rate have been reported to facilitate recovery from direct G protein regulation [19], we therefore investigated the effects of the W1684R and V1696I FHM-1 mutations on voltage-dependent Gβγ-mediated inhibition of recombinant $Ca_V2.1$ channels.

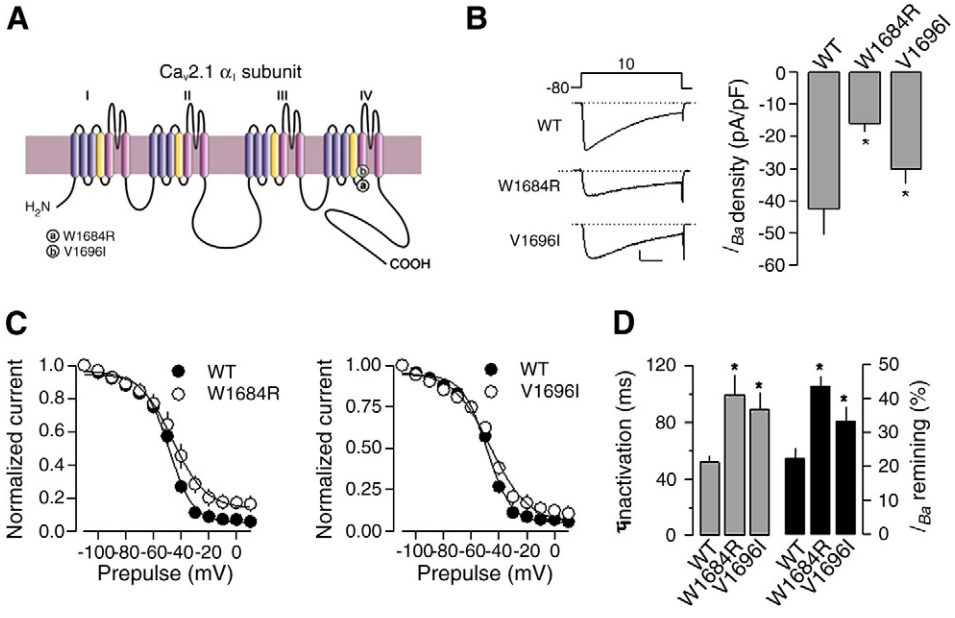

Fig. 1. FHM-1 mutations W1684R and V1696I may affect recombinant $Ca_V2.1$ channel activity in HEK-293 cells A: Locations of the two mutations in the secondary structure of the $Ca_V2.1\alpha_1$ subunit. B: Left panel, representative currents illustrating the magnitude and kinetics of WT (top trace) and W1684R (middle trace) and V1696I (bottom trace) channels obtained by applying depolarizing pulses to +10 mV during 250 ms from a holding potential (V_h) of −80 mV. Scale bar: 200 pA; 50 ms. Right panel, average percentage of current density WT and mutant channels; currents obtained as indicated in the left panel were normalized to cell capacitance (C_m). $n = 10–12$ recorded cells. C: Steady-state inactivation curves of currents through WT or mutant channels as indicated. Currents were elicited by a 2-s conditioning pulse from a V_h of −80 mV in 10 mV steps from −90 to +40 mV followed by a test pulse to +10 mV. The individual data points are means of 6–8 recorded cells. Error bars reflect standard errors, and the solid lines reflect fits via a Boltzmann function. $V_{1/2}$ values were −47.55, −39.49 and −43.89 mV for WT and FHM-1 mutant W1684R and V1696I channels, respectively. D: Comparison of time constant of inactivation (left panel) and percentage of current remaining (right panel) at the end of the 140-ms voltage-step (I_{rem}) in cells expressing WT and FHM-1 mutant channels. $n = 10–12$; *$P < 0.05$.

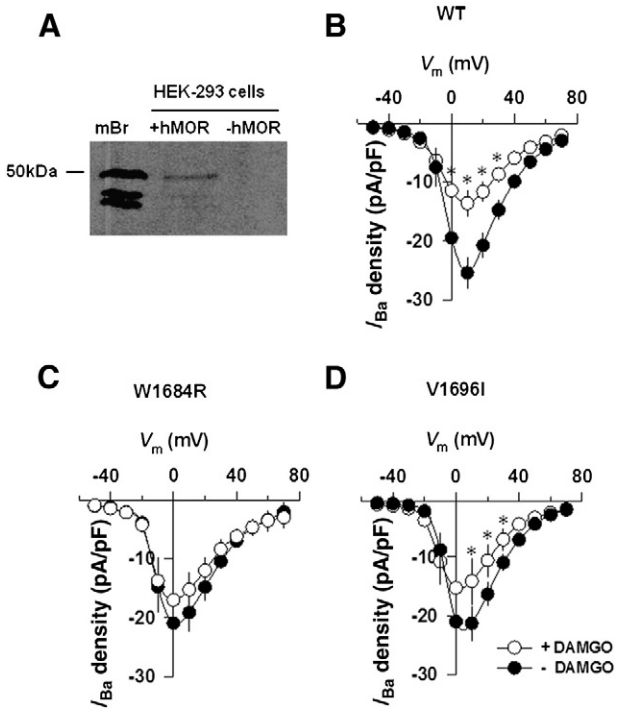

Fig. 2. Receptor-mediated G-protein regulation of WT and FHM-1 W1684R and V1696I mutant channels. A: Western blotting with a hMOR antibody on membranes from HEK-293 cells transfected with the $Ca_V2.1\alpha_1/Ca_V\alpha_2\delta$-1/$Ca_V\beta$ P/Q-type channel and the human μ-opioid receptor (+hMOR); untransfected cells (−hMOR) and mouse brain lysate (mBr) were used as controls. Data are representative of three independent experiments. B–D: Current density–voltage relationships for WT, W1684R and V1696I channels expressed in HEK-293 cells (n = 8–10 recoded cells) in the absence and presence of DAMGO as indicated. The asterisks denote statistically significant differences (*P<0.05).

To this end, recordings were then performed and current amplitude was examined after co-expressing the μ-opioid receptor (hMOR) using [D-Ala2, N-MePhe4, Gly-ol]-enkephalin (DAMGO), a synthetic opioid peptide with high specificity for hMOR. It is well known that hMORs couple to pertussis toxin (PTX)-sensitive G_i/G_o G-proteins to inhibit Ca^{2+} channels [32].

I_{Ba} was recorded from HEK-293 cells transiently transfected with either WT or FHM-1 mutant channels together with hMOR. Expression of hMOR was examined by Western blot analysis using a commercially available polyclonal antibody raised against a synthetic peptide derived from an internal region of the receptor (see Materials and methods). Fig. 2A shows that hMOR immunoreactivity was present both in the mouse brain (used as a positive control) and in hMOR-transfected HEK-293 cells. The identity of the labeled protein band as hMOR was confirmed by the expected size of the protein which migrated at an apparent molecular mass of ~50 kDa in 10% SDS-PAGE and the absence of staining when HEK-293 cells were mock-transfected.

Functional studies showed that exposure to 10 μM of DAMGO produced a rapid (within 10 s) voltage-dependent inhibition of the current through WT $Ca_V2.1\alpha_1/Ca_V\beta_3/\alpha_2\delta$-1 channels of about 50% (Fig. 2B). The inhibition was also present at the peak I_{Ba} (0 to + 10 mV) in both WT and FHM-1 mutant channel expressing cells (Fig. 2C and D); though DAMGO reduced I_{Ba} only ~20% in cells expressing W1684R or V1696I mutant channels. As current amplitudes were measured at their peak, these differences may reflect facilitated recovery from G protein inhibition occurring during membrane depolarization, therefore occurring between the start of the depolarization and the time to peak of the current [19].

One key feature of G protein modulation of Ca_V channels is its transient relief by a strong depolarizing prepulse. This phenomenon called facilitation is attributed to the dissociation of Gβγ dimers as channels undergo conformational changes in response to depolarization [18–20]. We took advantage of it to explore whether FHM-1 mutations alter the recovery from G protein mediated channel inhibition. Fig. 3B shows current traces through WT or mutant channels recorded during inhibition by DAMGO and elicited by 25-ms test pulses to the indicated potentials before (P1) and after (P2) the prepulse (PP) to +100 mV (Fig. 3A). Co-expression of $Ca_V2.1\alpha_1$ WT or the FHM-1 mutations together with $Ca_V\beta_3$ and $Ca_V\alpha_2\delta$-1 subunits in HEK-293 cells resulted in current facilitation (larger P2 than P1 currents following the PP), reflecting the voltage-dependent relief of Gβγ-mediated channel inhibition.

Notably, in the presence of DAMGO the amplitudes of the currents through WT and FHM-1 mutant channels were facilitated at test potentials ranging from −10 to +20 mV (not shown). However, a clear difference in the magnitude of facilitation was observed. Both WT and mutant channels exhibited maximum facilitation at 0 mV, which was 1.58 ± 0.12 for WT, 1.36 ± 0.06 for W1684R and 1.39 ± 0.07 for V1696I channels. The biggest reduction in facilitation was observed at +10 mV. At this potential, facilitation was significantly reduced from 1.47 ± 0.05 in the WT condition to 1.11 ± 0.03 and 1.36 ± 0.03 for W1684R and V1696I channels, respectively (Fig. 3C).

The lower level of DAMGO-mediated inhibition observed for the W1684R and V1696I mutant channels (Fig. 2) associated to a smaller extent of facilitation (Fig. 3), is consistent with changes in the

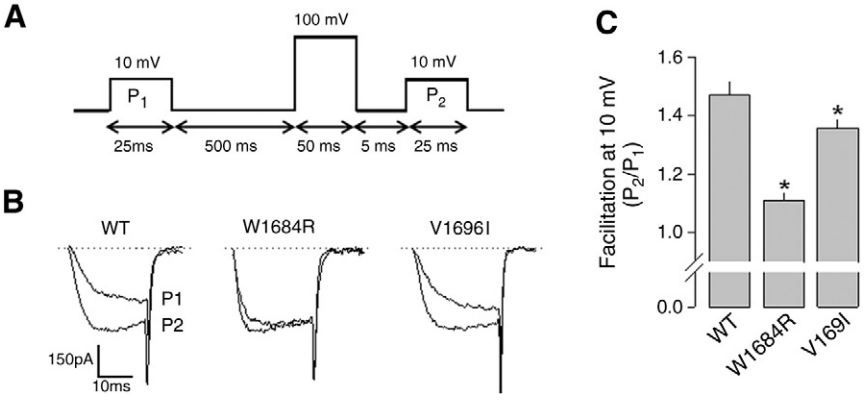

Fig. 3. FHM-1 mutations W1684R and V1696I alter G protein-mediated channel regulation. A: Depolarizing prepulse protocol used to relieve voltage-dependent G protein inhibition. The protocol consists of a voltage-step to +10 mV both before (P1) and after (P2) a depolarizing prepulse to +100 mV. B: Representative currents recorded during inhibition by 10 μm DAMGO before (P1) and after (P2) a 50-ms depolarizing prepulse to +100 mV. Test depolarizations to the indicated potential were given 500 ms before and 5 ms after the prepulse. Currents are superposed to facilitate comparison. C: Comparison of prepulse current facilitation recorded at 0 mV from cells expressing WT, W1684R and V1696I channels. Currents after the prepulse were normalized to the maximal current amplitude before the prepulse and then averaged. The histograms represent mean current amplitude facilitation versus test potential. n = 12–28 recorded cells; *P<0.05.

$Ca_V2.1\alpha_1$ subunit that result in alterations in the Gβγ-mediated inhibitory pathway. It is worth mentioning that one of the major inhibitory pathways controlling Ca_V channel activity at the synaptic level is mediated precisely by G-protein coupled receptor activation. In this context, the FHM-1 mutations may contribute to maintain Ca^{2+} influx through $Ca_V2.1$ channels especially during high synaptic activity by promoting channel de-inhibition.

Combined, the two parameters mentioned above reflect either, i) a lower level of Gβγ-mediated inhibition on the mutant channels, or ii) a facilitated de-inhibition during the test pulse at higher voltages. Therefore, we sought to determine the mechanism underlying this difference. To this end, we evaluated the time course for re-inhibition (at −80 mV) following facilitatory depolarization (facilitation decay) and for relief from inhibition (at +100 mV; facilitation onset), reflecting the association and dissociation rates of Gβγ dimers to/from the channel, respectively. The time constants for the onset and decay of facilitation can be measured by varying the parameters of the three-pulse voltage protocol. To monitor the onset of facilitation, the ratio of current amplitudes measured before and after the prepulse was plotted as a function of the conditioning pulse duration (Fig. 4A and B). For each cell, facilitation was fitted by a single exponential to obtain a time constant (τ dissociation; Fig. 4C). As can be seen in Fig. 4D, facilitation developed with an averaged time constant of 4.9 ± 0.5 ms for WT, 2.1 ± 0.5 ms and 3.8 ± 1.1 ms for W1684R and V1696I FHM-1 mutant channels, respectively. These results indicate that both FHM-1 mutations favor G protein dissociation from the channel during membrane depolarization.

The decay of facilitation was monitored by plotting the ratio of current amplitudes measured before and after the prepulse as a function of a variable interval between the conditioning prepulse and the second test pulse (Fig. 5A and B). For each cell, the decay of facilitation was fitted by a single exponential to obtain a time constant (τ re-association; Fig. 5C). Facilitation decayed with an averaged time constant of 27.8 ± 2.7 ms for WT, 15.2 ± 3.1 ms and 10.5 ± 1.0 ms for W1684R and V1696I channels, respectively (Fig. 5D).

It is well established that the onset and decay of prepulse facilitation during Gβγ-induced inhibition can be represented by a simple two-state model (Fig. 6A) [18,33–35], where $Ca_V2.1\alpha_1$ corresponds to the closed state of the channel, k_{on} is the association kinetic constant and k_{off} is the dissociation kinetic constant, both of them likely to have intrinsic voltage dependencies. During a facilitating depolarization to +100 mV, the Gβγ dimers should dissociate from the channels (Fig. 4). If Gβγ subunits do not also rebind channels during the depolarization, then k_{off} can be approximated by $1/\tau_{off}$. On repolarization to −80 mV, Gβγ dimers should rebind to channels at a rate equal to $k_{on}[G\beta\gamma] + k_{off}$. If at resting the inhibition of the channels by the Gβγ dimers is strong, as suggested by the results in Fig. 4, then k_{off} should be small, and k_{on} [Gβγ] can be approximated by $1/\tau_{on}$ [36].

Our results revealed that the time constants for Gβγ dissociation were different for WT and W1684R mutant channels (Fig. 4). Although our measurements reflect only the Gβγ association rate to the closed channel and the dissociation rate from the open channel, and do not allow an analysis at intermediate conformational states, the results clearly show that both mutations accelerates Gβγ dissociation from the channel. Hence, the estimated off-rate [k_{off} (s^{-1})] in our kinetic analysis was ~204 for the WT $Ca_V2.1\alpha_1$ subunit and ~261 and ~483 for the W1684R and V1696I mutant subunits, respectively, with a relative increase of ~1.3 and 2.4 fold (Fig. 6B). On the other hand, assuming an intracellular concentration of 50 nM for the Gβγ dimer [35], as well as that the interaction with the channels

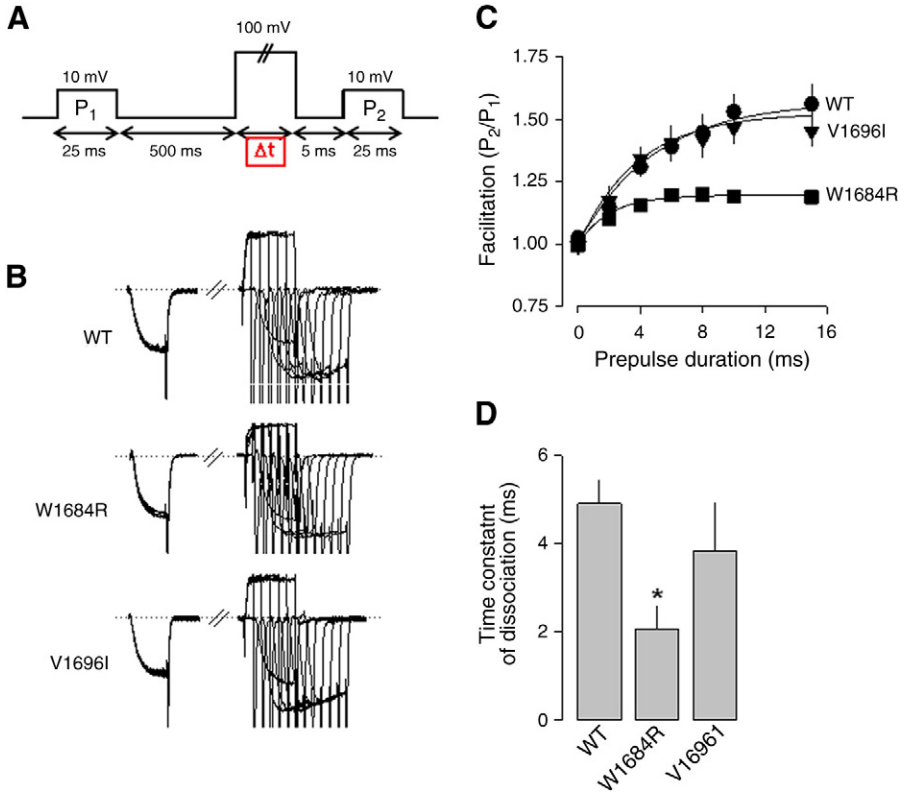

Fig. 4. FHM-1 mutations W1684R and V1696I accelerate the apparent rate of G protein dissociation from $Ca_V2.1$ channels. A: Depolarizing prepulse protocol used to study voltage-dependent G protein dissociation from the channel. Prepulse duration varied from 2 to 15 ms, and the interpulse intervals were fixed to 500 and 5 ms. Successive episodes of this voltage protocol were delivered at 20-s intervals. B: Representative current traces recorded during inhibition by 10 μm DAMGO of relief of G-protein regulation (facilitation development) recorded from HEK-293 cells expressing the WT, W1684R and V1696I channels. C: Comparison of time course of facilitation development (P2/P1 ratio) as a function of facilitatory prepulse duration for WT and FHM-1 mutant channels. D: Comparison of the time constant of G protein dissociation from WT and FHM-1 mutant channels. $n = 10–15$ recorded cells; *$P < 0.05$.

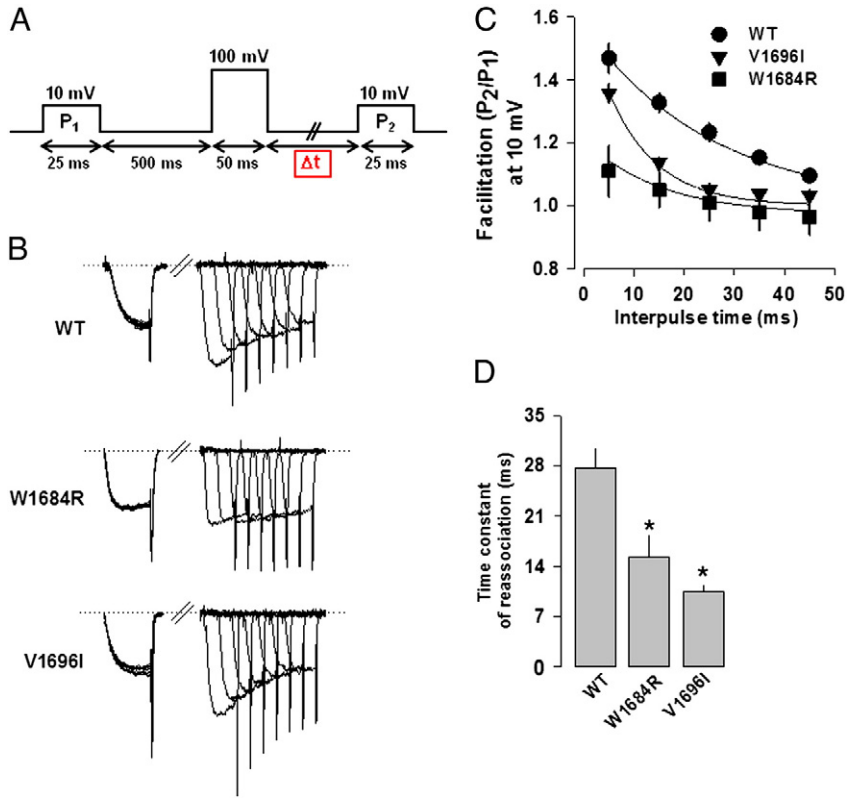

Fig. 5. FHM-1 mutation V1696I slows down the apparent rate of G protein association from P/Q channels. A: Depolarizing prepulse protocol used to study voltage-dependent G protein reassociation to the channel. The interval between the first test pulse, P1, and the prepulse (PP) was 500 ms; the interval between PP and the second test pulse, P2, (Δt) varied from 5 to 45 ms. B: Representative current traces recorded during inhibition by 10 μm DAMGO of re-inhibition by G proteins (facilitation decay) of WT and FHM-1 mutant channels, as indicated. Successive episodes of this voltage protocol were delivered at 20-s intervals. C: Comparison of time course of facilitation decay (P2/P1 ratio) as a function of interpulse duration for WT and FHM-1 mutant channels. D: Comparison of the time constant of G protein dissociation from WT and FHM-1 mutant channels. $n = 10–11$ recorded cells; *$P<0.05$.

occurs to a stoichiometric ratio of 1:1, the estimated on-rate [k_{on} [Gβγ] (s^{-1})] was 0.7, 1.3 and 1.9×10^9 ($M^{-1}\,s^{-1}$) for the WT, the W1684R and the V1691I subunits, respectively. These alterations in kinetics may help explain the apparent reduced voltage-dependent inhibition by G proteins of the $Ca_V2.1$ mutant channels.

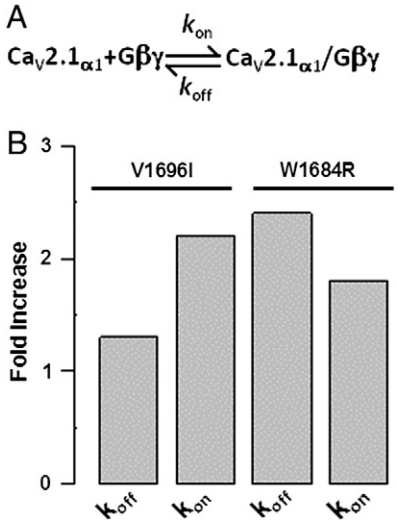

Fig. 6. FHM-1 mutations W1684R and V1696I alter the kinetics of prepulse facilitation. A: Simple kinetic scheme representing the binding of the Gβγ dimer of G-proteins to WT and FHM-1 mutant $Ca_V2.1\alpha_1$ subunits. The channels are assumed to have G protein bound ($Ca_V2.1\alpha_1$/Gβγ) and unbound ($Ca_V2.1\alpha_1$ + Gβγ) states modulated by transition rates (K_{on} and K_{off}). Arrows represent transition rates between states. B: Estimated kinetic constant values for the FHM-1 mutations W1684R and V1696I normalized and plotted as fold change with respect to WT channels.

It is worth noting that there was a difference in the K_d of Gβγ binding to the FHM-1 (V1696I<WT<W1684R). Though the reason for the difference in the affinity of the Gβγ dimer for the mutant channels is presently unknown, it is tempting to speculate that differences like this might be related to electrostatic potential changes occurring in the channels due to the presence of the mutations. It is well-known that the electrostatic potential plays an important role in many biological processes including folding, conformational stability, enzyme activity and protein–ligand or protein–protein interactions [37–39].

Given that hydrophobic interactions and electrostatic complementarity are important for high-affinity interactions, we decided to model the segments 4 and 5 of domain IV as well as the cytoplasmic loop connecting these two transmembrane segments in the $Ca_V2.1\alpha_1$ subunit (where the studied mutations are located) and determine its electrostatic potential. Our analysis showed that the V1696I mutation did not result in any change in the electrostatic potential in the region analyzed. However, the electrostatic potential was drastically affected by the W1684R mutation (Fig. 7) due to the substitution of a nonpolar amino acid (tryptophan) for a polar one (arginine). Interestingly, patients bearing the W1684R mutation, but not the V1696I mutation, have been shown to exhibit cerebellar ataxia as part of their phenotype [6].

4. Discussion

$Ca_V2.1$ (P/Q-type) channels are abundant in the mammalian brain where they mediate Ca^{2+} influx across presynaptic and somatodendritic membranes, thereby triggering neurotransmitter release and other key neuronal responses [40]. Because of its high expression level in the brain, the pore-forming (α_{1A}) subunit of the $Ca_V2.1$

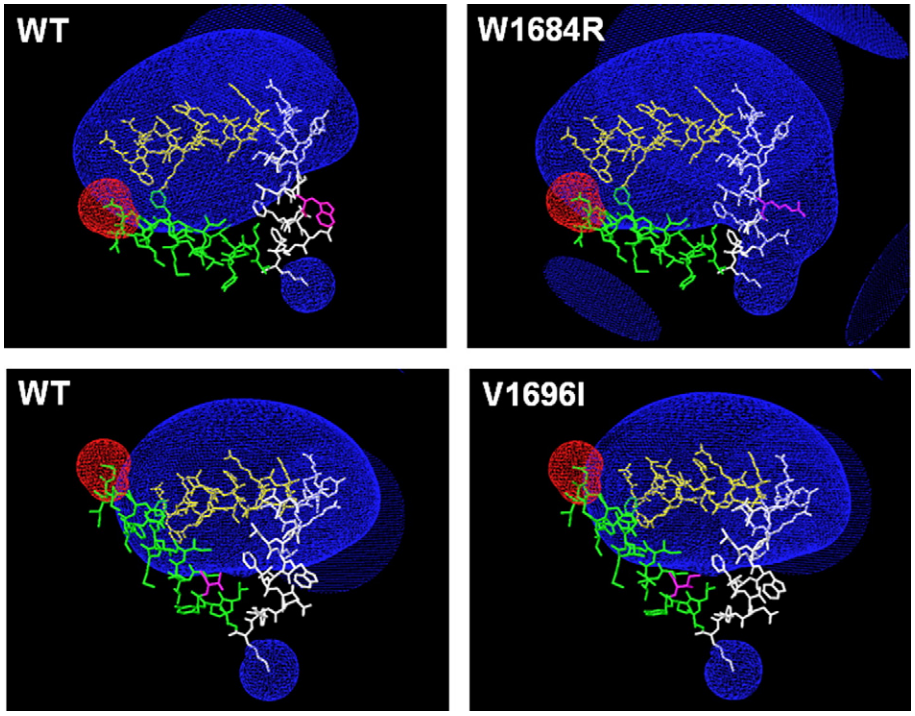

Fig. 7. Electrostatic potential distribution in the transmembrane segments 4 and 5 of domain IV of the $Ca_V2.1\alpha1$ channel subunit. The figure shows the most probable 3D model of the $Ca_V2.1\alpha1$ subunit motif IVS4 (yellow), IVS5 (green) and the cytoplasmic loop connecting both transmembrane segments (white). The electrostatic potential of the analyzed region in the wild-type sequence (WT) and in the two mutants (W1684R and V1696I) is shown in red (negative) and blue (positive). Tryptophan and valine in the WT sequence as well as arginine and isoleucine amino acid residues in the mutant channel sequences are all shown in magenta.

channel was the first representative of its class to be isolated by cDNA cloning [41,42]. Its importance also comes from the fact that mutations in the $Ca_V2.1\alpha_1$ subunit can cause neurological diseases such as FHM-1, episodic ataxia type 2 (EA-2) and spinocerebellar ataxia type 6 (SCA-6) [43,44].

Inhibition of $Ca_V2.1$ channels by G protein coupled receptors is widespread and is important for controlling neurotransmitter release. The complexity of this protein signaling mechanism is vast and involves distinct pathways that may converge on these channels. Perhaps the most prominent is the so-called voltage-dependent inhibition mediated by direct binding of the G protein βγ dimer to the $Ca_V2.1\alpha_1$ subunit of the channel [45-48]. Characteristic features of this modulation mechanism include a reduction in current amplitude, a slowdown in activation kinetics, and the development of prepulse facilitation during G protein regulation. These characteristics have been incorporated into models in which the $Ca_V2.1$ channels exhibit two functional gating states, "willing" and "reluctant" [48]. The reluctant channels are bound to Gβγ and display the voltage-dependent shifts in channel gating noted above.

Previous functional studies have investigated the response to G protein modulation of three different FHM-1 mutant channels [18–20]. Using recombinant $Ca_V2.1$ channels expressed in tsA-201 cells along with the dopamine D2 receptor, initial studies showed that the extent of G protein-mediated inhibition and the prepulse facilitation were reduced by the FHM-1 R192Q mutation. Since this mutation did not alter facilitation onset and decay or slow activation, it was suggested that the Gβγ-Ca_V channel affinity was not affected and that the consequences of the mutation were restricted to allosteric modifications that occurred after the Gβγ dimer bound to the channel [18]. More recently, we determined the functional consequences of, again, FHM-1 R192Q and mutation S218L mutations on G-protein regulation of $Ca_V2.1$ channels expressed in HEK-293 cells along with human μ-opioid receptors. Our results show that these mutations did not affect association of the Gβγ dimer onto the channel in the closed state but, in contrast to the results previously reported for R192Q, both mutations facilitated Gβγ dissociation from the activated channel, thereby decreasing the inhibitory G-protein pathway [19]. Similarly, more recently, it has been reported that also FHM-1 mutation Y1245C reduces G protein channel inhibition by favoring the dissociation of the Gβγ dimer from the channel [20].

Our data provide the first detailed evidence that W1684R and V1696I mutations cause conformational changes in the $Ca_V2.1\alpha_1$ subunit which result in alterations in the Gβγ-mediated inhibitory pathway. In particular, the results indicate that both FHM-1 mutations favor G protein dissociation from the channel during membrane depolarization. In a physiological context, this effect on G-protein regulation should contribute to render the neuronal network hyperexcitable, possibly as a consequence of reduced presynaptic inhibition, and help explain some aspects of the pathophysiology of FHM-1.

Likewise, studies in heterologous expression systems have shown that FHM-1 mutations may alter channel properties in a complex way, leading to both gain- and loss-of-function [10,11,49]. Our data suggest that the FHM-1 mutations W1684R and V1696I may influence $Ca_V2.1$ channels by affecting the dissociation of the Gβγ dimer. Although, a reduced channel density was observed in our data that could qualify as a possible mechanism (Fig. 1B), there is general consensus that a reduction of current density is more likely due to the method of heterologous expression given that no current reduction is observed when FHM-1 mutations are expressed in a more physiological environment, i.e. in knock-in mouse mutants [15,16]. Also the evidence that a reduction of mutant $Ca_V2.1$ expression results in EA-2, not FHM-1, would be in line with this.

Lastly, it is not entirely clear how alterations associated with FHM-1 mutations play a role in the pathogenesis of the disease, but a favored hypothesis considers neuronal hyperexcitability in the cerebral cortex as the basis for susceptibility to disease [50]. Although the effects of the W1684R and V1696I mutations on overall neuronal

excitability is difficult to predict, an increased postsynaptic excitability might result from this gain-of-function variants of presynaptic channels controlling release of excitatory neurotransmitters. Hence, in addition to altered response to direct G-protein regulation, it is possible that the mutations might interfere also with other molecular signaling important for neurotransmitter vesicle release. Though the two FHM-1 mutations reported here are located in conserved regions of the Cav2.1α_1 subunit (Fig. 1A) where no interaction sites with proteins of the exocytotic machinery has been reported, the possibility exists, that the altered responses of the mutant channels to G-protein regulation could result from inappropriate indirect interactions with such proteins. This is an interesting topic for future studies.

Supplementary related to this article can be found online at http://dx.doi.org/10.1016/j.bbadis.2012.04.008.

Acknowledgements

We gratefully appreciate the technical expertise of G. Aguilar and M. Urbán. This work was supported in part by grants from Conacyt to R.F. (128707) and PAPIIT to A.S. (IN221011). Doctoral and Postdoctoral fellowships from Conacyt to E.G.L., M.A.G. and R.G.R. are gratefully acknowledged. The authors would like to thank the two anonymous reviewers for their helpful comments and suggestions.

References

[1] P.J. Goadsby, R.B. Lipton, M.D. Ferrari, Migraine — current understanding and treatment, N. Engl. J. Med. 346 (2002) 257–270.
[2] V. Anttila, H. Stefansson, M. Kallela, U. Todt, G.M. Terwindt, M.S. Calafato, D.R. Nyholt, A.S. Dimas, T. Freilinger, B. Müller-Myhsok, V. Artto, M. Inouye, K. Alakurtti, M.A. Kaunisto, E. Hämäläinen, B. De Vries, A.H. Stam, C.M. Weller, A. Heinze, K. Heinze-Kuhn, I. Goebel, G. Borck, H. Göbel, S. Steinberg, C. Wolf, A. Björnsson, G. Gudmundsson, M. Kirchmann, A. Hauge, T. Werge, T. Schoenen, J.G. Eriksson, K. Hagen, L. Stovner, H.E. Wichmann, T. Meitinger, M. Alexander, S. Moebus, S. Schreiber, Y.S. Aulchenko, M.M. Breteler, A.G. Uitterlinden, A. Hofman, C.M. Van Duijn, P. Tikka-Kleemola, S. Vepsäläinen, S. Lucae, F. Tozzi, P. Muglia, J. Barrett, J. Kaprio, M. Färkkilä, L. Peltonen, K. Stefansson, J.A. Zwart, M.D. Ferrari, J. Olesen, M. Daly, M. Wessman, A.M. Van den Maagdenberg, M. Dichgans, C. Kubisch, E.T. Dermitzakis, R.R. Frants, A. Palotie, on behalf of the International Headache Genetics Consortium, Genome-wide association study of migraine implicates a common susceptibility variant on 8q22.1, Nat. Genet. 42 (2010) 869–873.
[3] D.I. Chasman, M. Schürks, V. Anttila, B. De Vries, U. Schminke, L.J. Launer, G.M. Terwindt, A.M. Van den Maagdenberg, K. Fendrich, H. Völzke, F. Ernst, L.R. Griffiths, J.E. Buring, M. Kallela, T. Freilinger, C. Kubisch, P.M. Ridker, A. Palotie, M.D. Ferrari, W. Hoffmann, R.Y. Zee, T. Kurth, Genome-wide association study reveals three susceptibility loci for common migraine in the general population, Nat. Genet. 43 (2011) 695–698.
[4] M.D. Ferrari, A.M. Van den Maagdenberg, R.R. Frants, P.J. Goadsby, Migraine as a cerebral ionopathy with impaired central sensory processing, in: S.G. Waxman (Ed.), Molecular Neurology, Elsevier, Amsterdam, 2007, pp. 439–461.
[5] S. Rajakulendran, D. Kaski, M.G. Hanna, Neuronal P/Q-type calcium channel dysfunction in inherited disorders of the CNS, Nat. Rev. Neurol. 8 (2012) 86–96.
[6] A. Ducros, C. Dernier, A. Joutel, M. Cecillon, C. Lescoat, K. Vahedi, F. Darcel, E. Vicaut, M.G. Bousser, E. Tournier-Lasserve, The clinical spectrum of familial hemiplegic migraine associated with mutations in a neuronal calcium channel, N. Engl. J. Med. 354 (2001) 17–24.
[7] B. De Vries, R.R. Frants, M.D. Ferrari, A.M. Van den Maagdenberg, Molecular genetics of migraine, Hum. Genet. 126 (2009) 115–132.
[8] R. Felix, Calcium channelopathies, Neuromolecular Med. 8 (2006) 307–318.
[9] D. Pietrobon, Familial hemiplegic migraine, Neurotherapeutics 4 (2007) 274–284.
[10] O.D. Uchitel, C.G. Inchauspe, F.J. Urbano, M.N. Di Guilmi, $Ca_V2.1$ voltage activated calcium channels and synaptic transmission in familial hemiplegic migraine pathogenesis. J. Physiol. Paris (in press).
[11] D. Pietrobon, Insights into migraine mechanisms and $Ca_V2.1$ calcium channel function from mouse models of familial hemiplegic migraine, J. Physiol. 588 (2010) 1871–1878.
[12] M. Hans, S. Luvisetto, M.E. Williams, M. Spagnolo, A. Urrutia, A. Tottene, P.F. Brust, E.C. Johnson, M.M. Harpold, K.A. Stauderman, D. Pietrobon, Functional consequences of mutations in the human α_{1A} calcium channel subunit linked to familial hemiplegic migraine, J. Neurosci. 19 (1999) 1610–1619.
[13] A. Tottene, T. Fellin, S. Pagnutti, S. Luvisetto, J. Striessnig, C. Fletcher, D. Pietrobon, Familial hemiplegic migraine mutations increase Ca^{2+} influx through single human $Ca_V2.1$ channels and decrease maximal $Ca_V2.1$ current density in neurons, Proc. Natl. Acad. Sci. U. S. A. 99 (2002) 13284–13289.
[14] C.F. Barrett, Y.Q. Cao, R.W. Tsien, Gating deficiency in a familial hemiplegic migraine type 1 mutant P/Q-type calcium channel, J. Biol. Chem. 280 (2005) 24064–24071.
[15] A.M. Van den Maagdenberg, D. Pietrobon, T. Pizzorusso, S. Kaja, L.A. Broos, T. Cesetti, R.C. Van de Ven, A. Tottene, J. Van der Kaa, J.J. Plomp, R.R. Frants, M.D. Ferrari, A Cacna1a knockin migraine mouse model with increased susceptibility to cortical spreading depression, Neuron 41 (2004) 701–710.
[16] A.M. Van den Maagdenberg, T. Pizzorusso, S. Kaja, N. Terpolilli, M. Shapovalova, F.E. Hoebeek, C.F. Barrett, L. Gherardini, R.C. Van de Ven, B. Todorov, L.A. Broos, A. Tottene, Z. Gao, M. Fodor, C.I. De Zeeuw, R.R. Frants, N. Plesnila, J.J. Plomp, D. Pietrobon, M.D. Ferrari, High cortical spreading depression susceptibility and migraine-associated symptoms in $Ca_V2.1$ S218L mice, Ann. Neurol. 67 (2010) 85–98.
[17] A. Tottene, R. Conti, A. Fabbro, D. Vecchia, M. Shapovalova, M. Santello, A.M. van den Maagdenberg, M.D. Ferrari, D. Pietrobon, Enhanced excitatory transmission at cortical synapses as the basis for facilitated spreading depression in $Ca_V2.1$ knockin migraine mice, Neuron 61 (2009) 762–773.
[18] K. Melliti, M. Grabner, G.R. Seabrook, The familial hemiplegic migraine mutation R192Q reduces G-protein-mediated inhibition of P/Q-type ($Ca_V2.1$) calcium channels expressed in human embryonic kidney cells, J. Physiol. 546 (2003) 337–347.
[19] N. Weiss, A. Sandoval, R. Felix, A. Van den Maagdenberg, M. De Waard, The S218L familial hemiplegic migraine mutation promotes deinhibition of $Ca_V2.1$ calcium channels during direct G-protein regulation, Pflugers Arch. 457 (2008) 315–326.
[20] S.A. Serra, N. Fernandez-Castillo, A. Macaya, B. Cormand, M.A. Valverde, J.M. Fernandez-Fernandez, The hemiplegic migraine-associated Y1245C mutation in CACNA1A results in a gain of channel function due to its effect on the voltage sensor and G-protein-mediated inhibition, Pflugers Arch. 458 (2009) 489–502.
[21] M. Hans, A. Urrutia, C. Deal, P.F. Brust, K. Stauderman, S.B. Ellis, M.M. Harpold, E.C. Johnson, M.E. Williams, Structural elements in domain IV that influence biophysical and pharmacological properties of human α_{1A}-containing high-voltage-activated calcium channels, Biophys. J. 76 (1999) 1384–1400.
[22] A. Castellano, X. Wei, L. Birnbaumer, E. Perez-Reyes, Cloning and expression of a neuronal calcium channel β subunit, J. Biol. Chem. 268 (1993) 12359–12366.
[23] H.L. Kim, H. Kim, P. Lee, R.G. King, H. Chin, Rat brain expresses an alternatively spliced form of the dihydropyridine-sensitive L-type calcium channel α_2 subunit, Proc. Natl. Acad. Sci. U. S. A. 89 (1992) 3251–3255.
[24] C. Müllner, L.A. Broos, A.M. Van den Maagdenberg, J. Striessnig, Familial hemiplegic migraine type 1 mutations K1336E, W1684R, and V1696I alter $Ca_V2.1$ Ca^{2+} channel gating: evidence for β-subunit isoform-specific effects, J. Biol. Chem. 279 (2004) 51844–51850.
[25] N. Weiss, A. Sandoval, S. Kyonaka, R. Felix, Y. Mori, M. De Waard, Rim1 modulates direct G-protein regulation of $Ca_V2.2$ channels, Pflugers Arch. 461 (2011) 447–459.
[26] R. Felix, C.A. Gurnett, M. De Waard, K.P. Campbell, Dissection of functional domains of the voltage-dependent Ca^{2+} channel $\alpha_2\delta$ subunit, J. Neurosci. 17 (1997) 6884–6891.
[27] M.A. Gandini, A. Sandoval, R. González-Ramírez, Y. Mori, M. de Waard, R. Felix, Functional coupling of Rab3-interacting molecule 1 (RIM1) and L-type Ca^{2+} channels in insulin release, J. Biol. Chem. 286 (2011) 15757–15765.
[28] O.P. Hamill, A. Marty, E. Neher, B. Sakmann, F.J. Sigworth, Improved patch-clamp techniques for high-resolution current recording from cells and cell-free membrane patches, Pflugers Arch. 391 (1981) 85–100.
[29] G. Avila, A. Sandoval, R. Felix, Intramembrane charge movement associated with endogenous K^+ channel activity in HEK-293 cells, Cell. Mol. Neurobiol. 24 (2004) 317–330.
[30] X. Chen, Q. Wang, F. Ni, J. Ma, Structure of the full-length Shaker potassium channel Kv1.2 by normal-mode-based X-ray crystallographic refinement, Proc. Natl. Acad. Sci. U. S. A. 107 (2010) 11352–11357.
[31] J. Liang, S. Subramaniam, Computation of molecular electrostatics with boundary element methods, Biophys. J. 73 (1997) 1830–1841.
[32] C.P. Bailey, M. Connor, Opioids: cellular mechanisms of tolerance and physical dependence, Curr. Opin. Pharmacol. 5 (2005) 60–68.
[33] K.P. Currie, A.P. Fox, Comparison of N- and P/Q- type voltage-gated calcium channel current inhibition, J. Neurosci. 17 (1997) 4570–4579.
[34] M.I. Arnot, S.C. Stotz, S.E. Jarvis, G.W. Zamponi, Differential modulation of N-type 1B and P/Q-type 1A calcium channels by different G protein subunit isoforms, J. Physiol. 527 (2000) 203–212.
[35] C. Cantí, Y. Bogdanov, A.C. Dolphin, Interaction between G proteins and accessory β subunits in the regulation of α1B calcium channels in *Xenopus* oocytes, J. Physiol. 527 (2000) 419–432.
[36] U. Meza, B. Adams, G-protein-dependent facilitation of neuronal α1A, α1B, and α1E Ca channels, J. Neurosci. 18 (1998) 5240–5252.
[37] S.D. Zakharov, J.B. Heymann, Y.L. Zhang, W.A. Cramer, Membrane binding of the colicin E1 channel: activity requires an electrostatic interaction of intermediate magnitude, Biophys. J. 70 (1996) 2774–2783.
[38] K.J. Schleifer, H.D. Höltje, Molecular modelling investigation of wild-type and the R528H mutated segment IIS4 of human L-type voltage-gated calcium channels, Protein Eng. 11 (1998) 1033–1040.
[39] A. Hildebrandt, R. Blossey, S. Rjasanow, O. Kohlbacher, H.P. Lenhof, Electrostatic potentials of proteins in water: a structured continuum approach, Bioinformatics 23 (2007) e99–e103.
[40] R.M. Evans, G.W. Zamponi, Presynaptic Ca^{2+} channels — integration centers for neuronal signaling pathways, Trends Neurosci. 29 (2006) 617–624.
[41] Y. Mori, T. Friedrich, M.S. Kim, A. Mikami, J. Nakai, P. Ruth, E. Bosse, F. Hofmann, V. Flockerzi, T. Furuichi, K. Mikoshiba, K. Imoto, T. Tanabe, S. Numa, Primary structure and functional expression from complementary DNA of a brain calcium channel, Nature 350 (1991) 398–402.
[42] T.V. Starr, W. Prystay, T.P. Snutch, Primary structure of a calcium channel that is highly expressed in the rat cerebellum, Proc. Natl. Acad. Sci. U. S. A. 88 (1991) 5621–5625.

[43] R.A. Ophoff, G.M. Terwindt, M.N. Vergouwe, R. Van Eijk, P.J. Oefner, S.M. Hoffman, J.E. Lamerdin, H.W. Mohrenweiser, D.E. Bulman, M. Ferrari, J. Haan, D. Lindhout, G.J. Van Ommen, M.H. Hofker, M.D. Ferrari, R.R. Frants, Familial hemiplegic migraine and episodic ataxia type-2 are caused by mutations in the Ca^{2+} channel gene CACNL1A4, Cell 87 (1996) 543–552.
[44] O. Zhuchenko, J. Bailey, P. Bonnen, T. Ashizawa, D.W. Stockton, C. Amos, W.B. Dobyns, S.H. Subramony, H.Y. Zoghbi, C.C. Lee, Autosomal dominant cerebellar ataxia (SCA6) associated with small polyglutamine expansions in the α1A-voltage-dependent calcium channel, Nat. Genet. 15 (1997) 62–69.
[45] M. De Waard, H. Liu, D. Walker, V.E. Scott, C.A. Gurnett, K.P. Campbell, Direct binding of G-protein βγ complex to voltage-dependent calcium channels, Nature 385 (1997) 446–450.
[46] G.W. Zamponi, E. Bourinet, D. Nelson, J. Nargeot, T.P. Snutch, Crosstalk between G proteins and protein kinase C mediated by the calcium channel alpha1 subunit, Nature 385 (1997) 442–446.
[47] K.P. Currie, G protein modulation of Ca_V2 voltage-gated calcium channels, Channels (Austin) 4 (2010) 497–509.
[48] H.W. Tedford, G.W. Zamponi, Direct G protein modulation of Ca_V2 calcium channels, Pharmacol. Rev. 58 (2006) 837–862.
[49] A.M. Van den Maagdenberg, J. Haan, G.M. Terwindt, M.D. Ferrari, Migraine: gene mutations and functional consequences, Curr. Opin. Neurol. 20 (2007) 299–305.
[50] N. Weiss, E. Tournier-Lasserve, M. De Waard, Role of P/Q calcium channel in familial hemiplegic migraine, Med Sci (Paris) 23 (2007) 53–63.